Supplementary Information (SI) for Journal of Materials Chemistry B.

A Self-Healing Injectable PF127-Gelatin Bioadhesive Sealant with Antioxidant and Antibacterial Activities for Accelerated Oral Ulcer Repair

Jinghan Wang,†[a,b] Gang He,†[c] Jinying Zhao,[c] Min Chen,[c] Zheng Pan,[c] Chong Zhang,*[c] Decheng Wu*[c], Wen Sui*[a]

[a]College of Pharmacy, College of Stomatology, Shenzhen Technology University, Shenzhen, Guangdong, 518118, China

[b]School of Pharmacy, Shenzhen University Medical School, Shenzhen University, Shenzhen, Guangdong, 518055, China

[c]Guangdong Provincial Key Laboratory of Advanced Biomaterials, Department of Biomedical Engineering, Southern University of Science and Technology, No. 1088 Xueyuan Avenue, Nanshan District Shenzhen, Guangdong 518055, China.

Email: zhangc9@sustech.edu.cn; wudc@sustech.edu.cn; suiwen@sztu.edu.cn

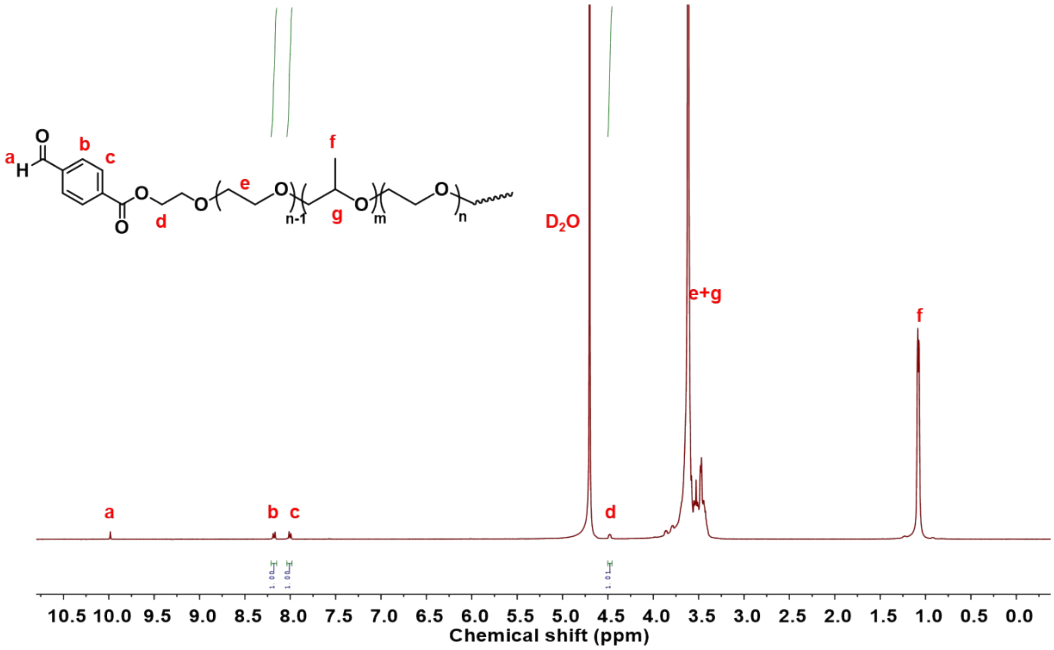

Fig. S1 ^{1}H NMR spectrum of the PF127-CHO.

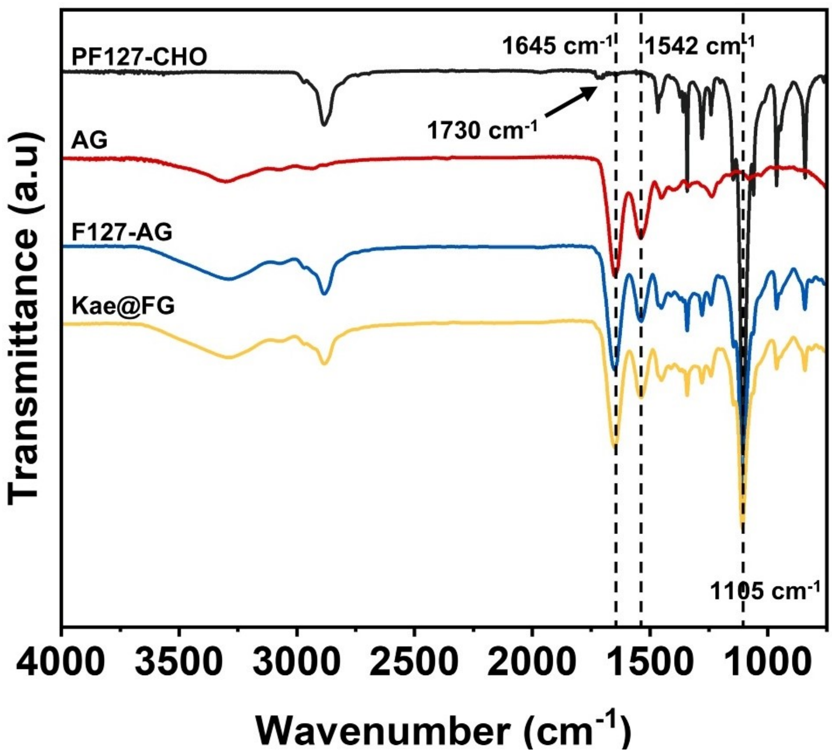

Fig. S2 FT-IR spectra of PF127-CHO, amino gelatin (AG), 20% (*w*/*v*) F127-AG hydrogel, and Kae@FG hydrogel.

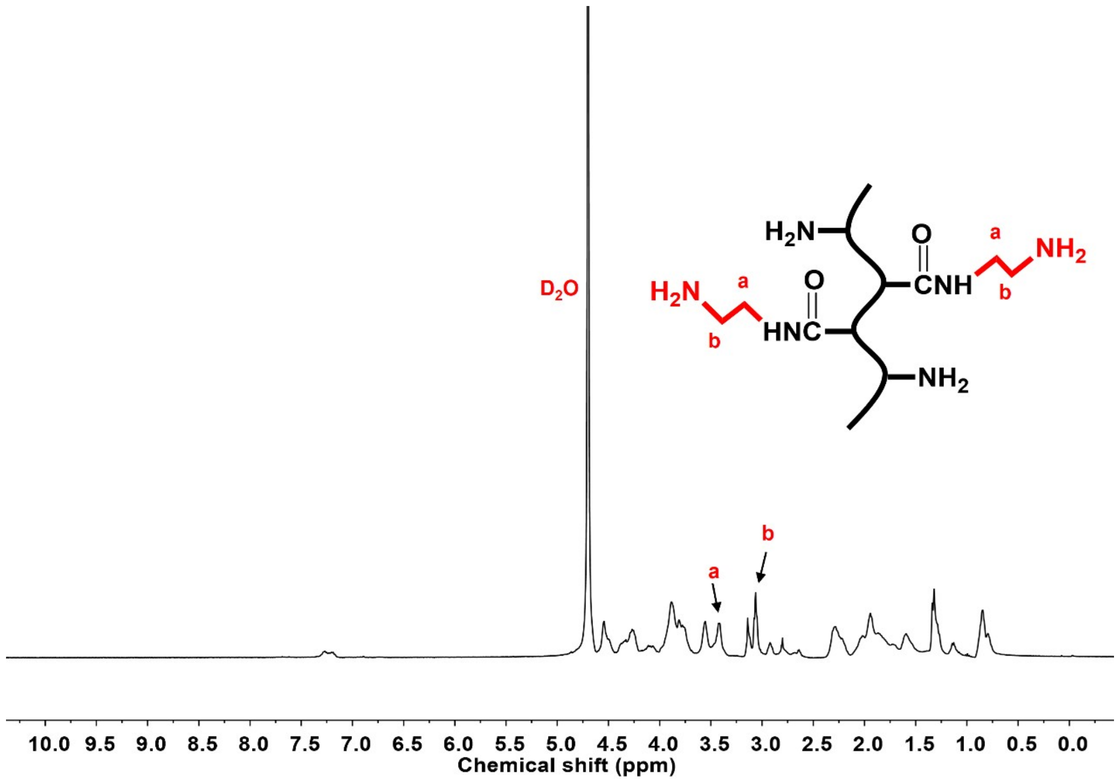

Fig. S3 ^{1}H NMR spectrum of the amino gelatin (AG)

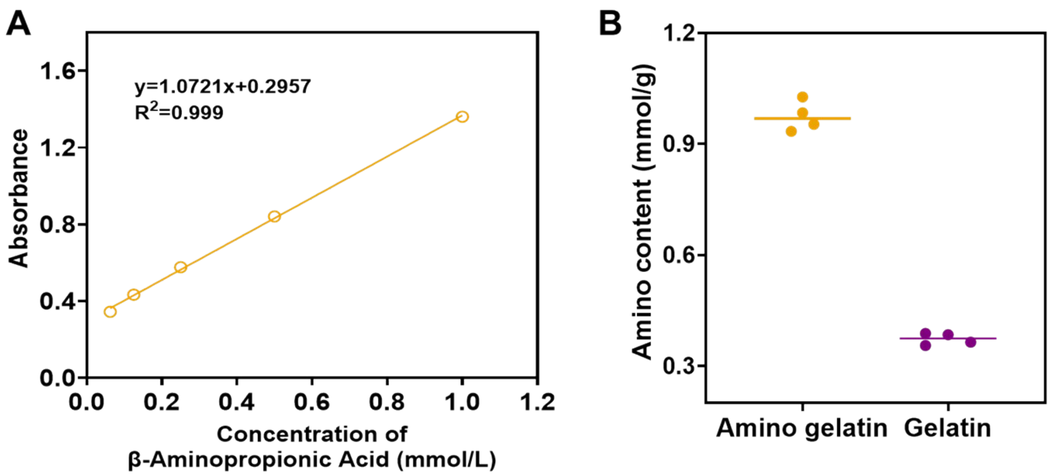

Fig. S4 Determination of free amino groups using the TNBS method. (A) Standard curve of β-aminopropionic acid. (B) Quantification of amino group content in unmodified gelatin and amino gelatin (AG) based on TNBS assay (n = 4).

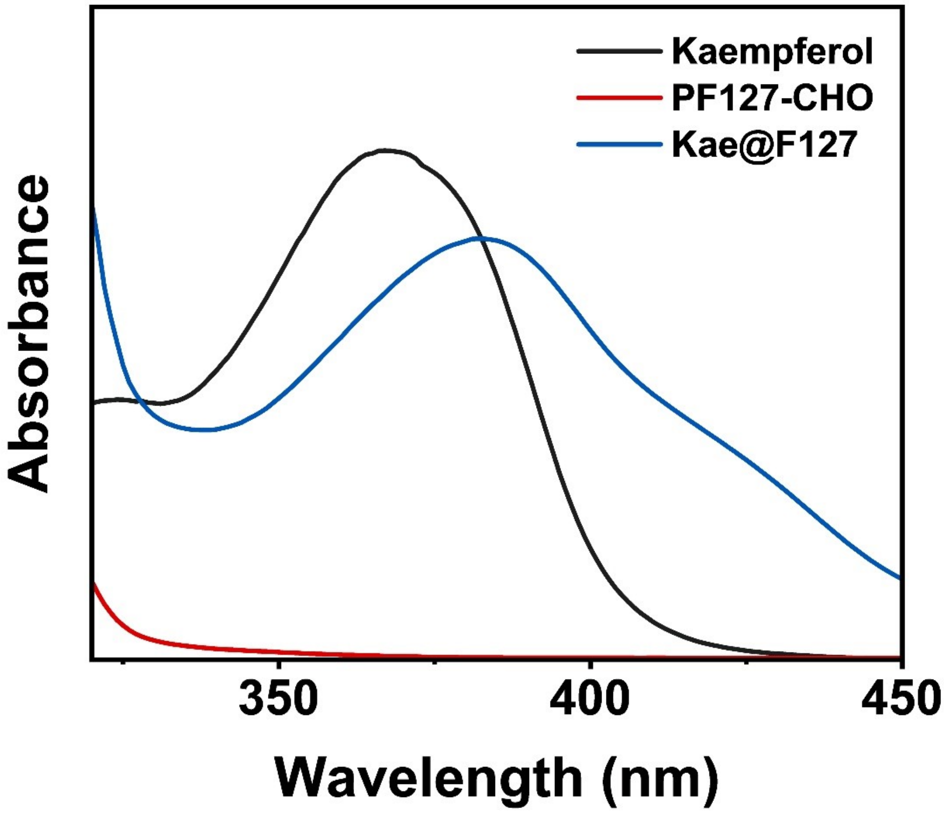

Fig. S5 UV-Vis absorption spectra of kaempferol, PF127-CHO, and Kae-loaded F127 (Kae@F127) solutions.

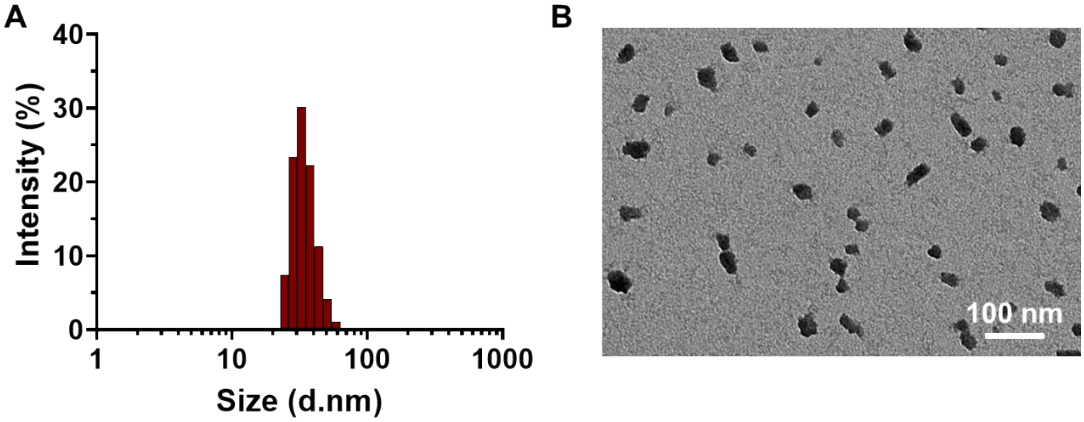

Fig. S6 (A) Particle size distribution of Kae@F127-CHO micelles and (B) representative TEM image of Kae@F127-CHO micelles (scale bar: 100 nm).

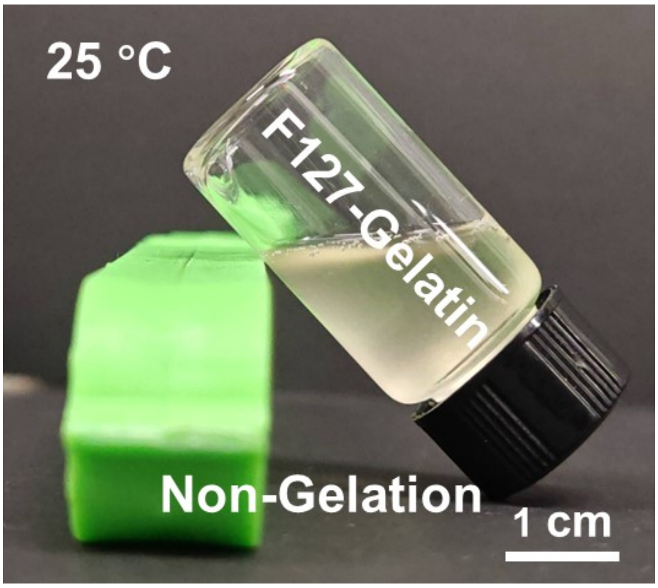

Fig. S7 Photograph of the mixture of equal volumes of unmodified gelatin and PF127-CHO, each at 20% (w/v), showing no gel formation (scale bar: 1 cm).

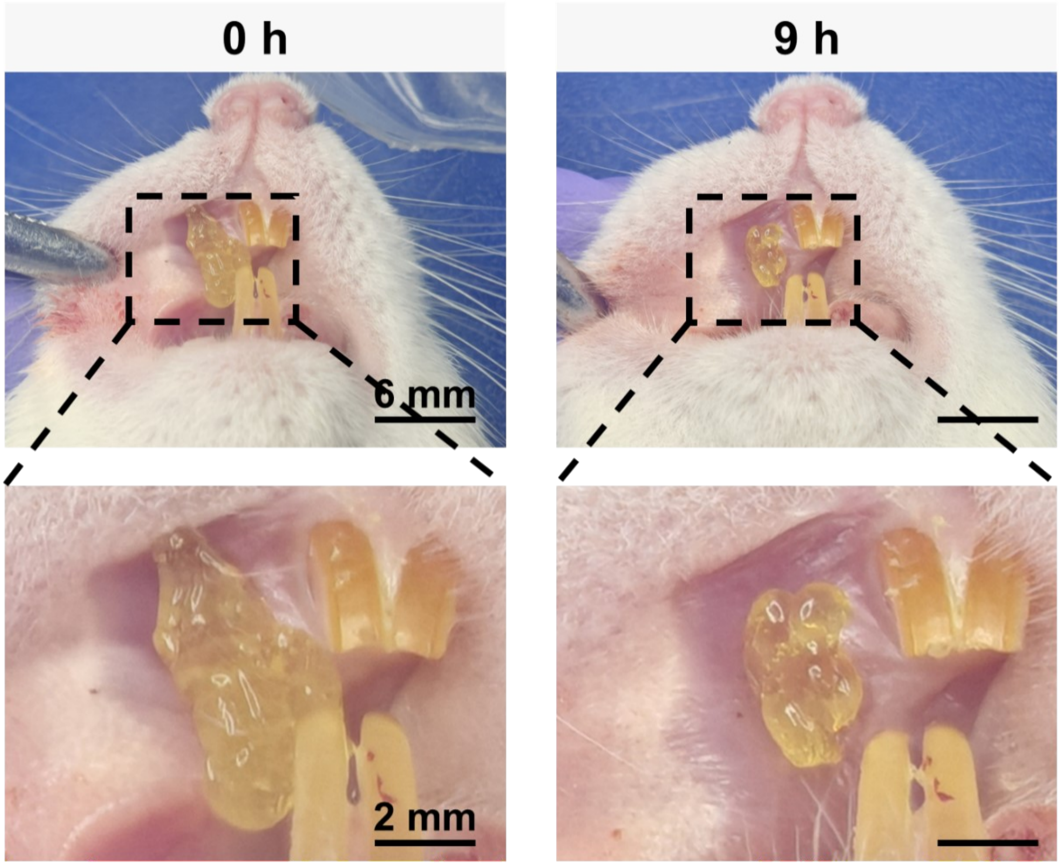

Fig. S8 Representative in vivo photographs showing the retention of Kae@FG hydrogel on the oral mucosa of SD rats (scale bar: 6 mm). High-magnification views of the indicated regions are also shown (scale bar: 2 mm).

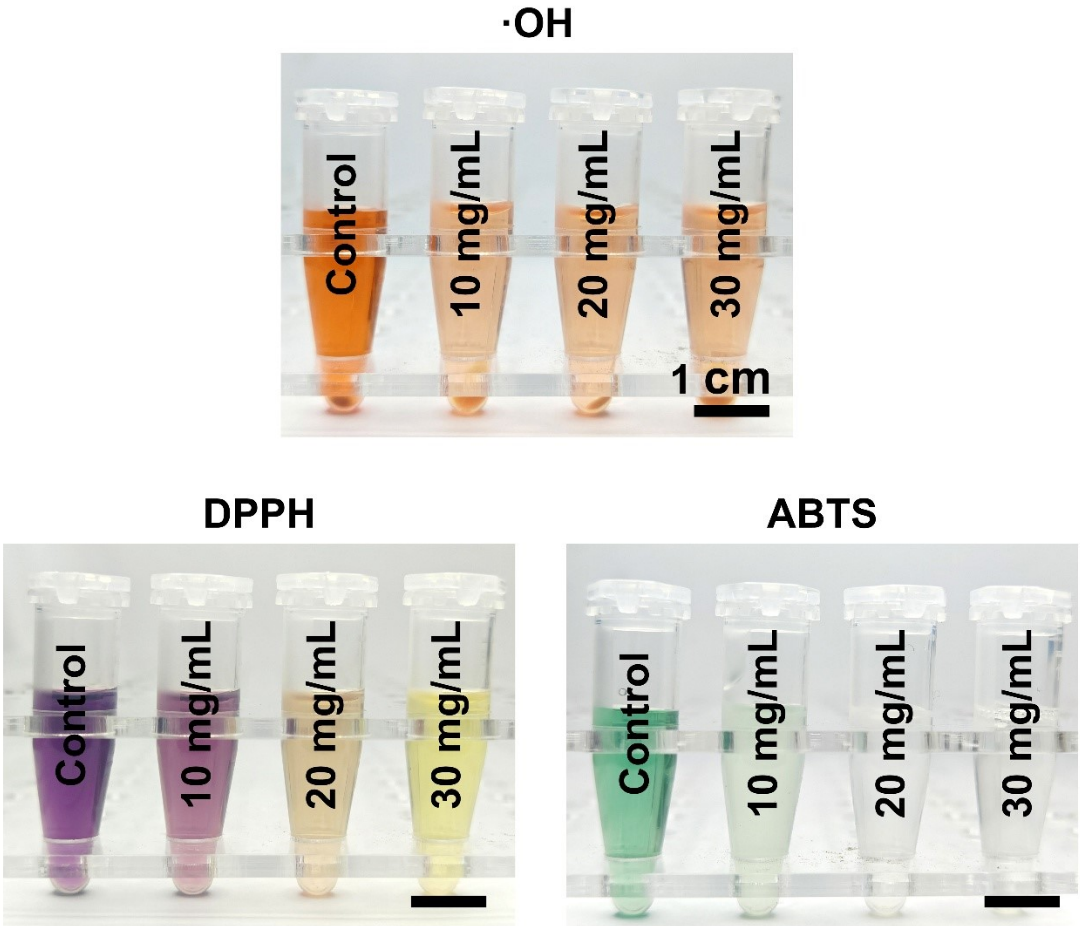

Fig. S9 Photographs showing color changes of ·OH, DPPH, and ABTS solutions after co-incubation with hydrogels at different concentrations (scale bar: 1 cm).

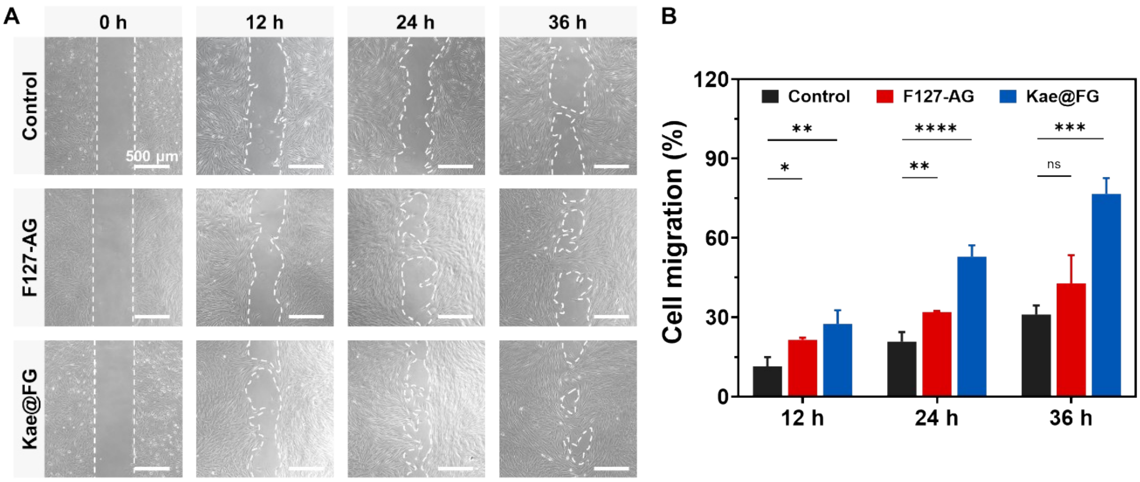

Fig. S10 Representative images (A) and quantitative analysis (B) of HGF cell migration under oxidative stress following treatment with hydrogel extracts from F127-AG and Kae@FG (scale bar: 500 μm, n = 3). Data are presented as mean ± S.D. Statistical analysis in (B) was performed by one-way ANOVA with Dunnett's multiple comparisons test (*$p < 0.05$, **$p < 0.01$, ***$p < 0.001$, ****$p < 0.0001$, *ns* = not significant).

Fig. S11 Representative photograph showing the establishment of the rat oral ulcer model (scale bar: 5 mm).

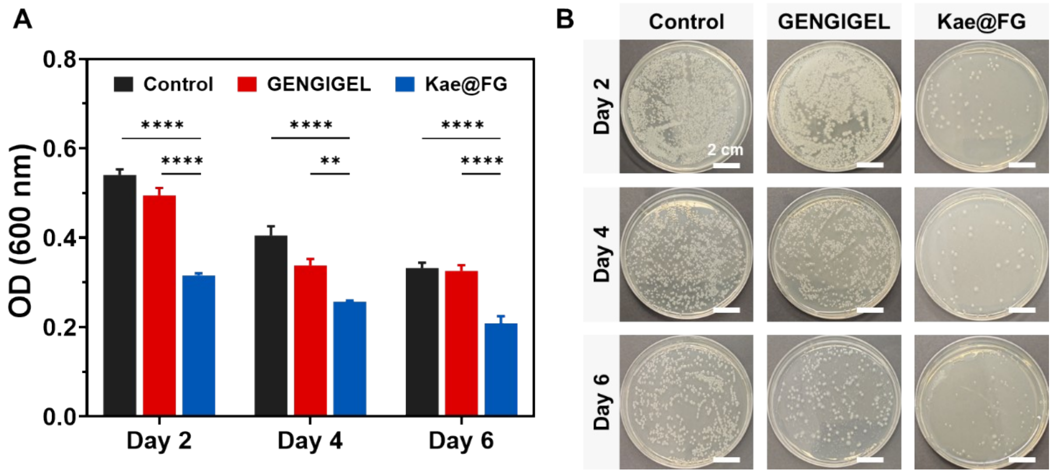

Fig. S12 The OD600 values of bacterial suspension (A) and bacterial colonies from different groups on days 2, 4 and 6 (B) (scale bar: 2 cm, n = 3). Data are presented as mean ± S.D. Statistical analysis in (A) was performed by one-way ANOVA with Dunnett's multiple comparisons test (**$p < 0.01$, ****$p < 0.0001$).

Table S1 List of primary and secondary antibodies used in this study

Primary Antibody	Catalog Number	Manufacturer	Species	Primary Antibody Dilution	Secondary Antibody	Secondary Antibody Dilution
TNF-α	GB11188	Servicebio	Rabbit	1:500	HRP-conjugated Goat Anti-Rabbit IgG	1:500
MPO	GB11224	Servicebio	Rabbit	1:1000	HRP-conjugated Goat Anti-Rabbit IgG	1:500
CD31	GB113151	Servicebio	Rabbit	1:500	HRP-conjugated Goat Anti-Rabbit IgG	1:500
iNOS	GB11119	Servicebio	Rabbit	1:500	HRP-conjugated Goat Anti-Rabbit IgG	1:500
CD206	GB113497	Servicebio	Rabbit	1:500	HRP-conjugated Goat Anti-Rabbit IgG	1:500
HO-1	GB115713	Servicebio	Rabbit	1:500	HRP-conjugated Goat Anti-Rabbit IgG	1:500